MESON PRODUCTION IN PHOTONUCLEAR, π-INDUCED AND HEAVY-ION REACTIONS: ELEMENTARY PROCESSES AND MEDIUM EFFECTS*

V. Metag

II. Physikalisches Institut, Universität Giessen
Heinrich Buff Ring 16, D-35392 Giessen, Germany

(Received January 26, 2000)

The structure of the nucleon has been investigated by studying the photoexcitation of nucleon resonances and their subsequent meson decay. The photon spectrometer TAPS has been used in a series of corresponding experiments at the Mainz microtron MAMI. A comparison of the photoproduction of mesons on the free nucleon and on nucleons bound in nuclei reveales differences attributed to changes in the properties of hadrons in the nuclear medium. Most of the nucleon resonances exhibit only a small shift in mass but an appreciable broadening. The largest effect is observed for the D_{13}-resonance which may be attributed to its ρ-meson decay. Various calculations predict a change in the spectral function of this vector meson in the nuclear medium. First experimental evidence for medium modifications of vector mesons may have been observed in ultra-relativistic heavy-ion collisions, *e.g.* with the CERES detector. A dedicated program focusing on the properties of mesons in the nuclear environment at different temperatures and baryon densities will be taken up with the HADES di-lepton spectrometer at GSI, utilizing the π- and heavy-ion beams from SIS. Photonuclear, hadron and heavy-ion induced reactions are thus complementary approaches to study the properties of hadrons in nuclear matter.

PACS numbers: 25.75.Dw, 25.20.–x, 25.80.Hp

1. Introduction

Nucleons and mesons have a complex substructure of valence quarks, gluons and quark-antiquark pairs. In most cases, the mass of a composite system is nearly equal to the sum of masses of the constituents. For atoms and nuclei, the binding forces among the constituents only cause a slight

* Invited talk presented at the NATO Advanced Research Workshop, Krzyże, Poland September 2–4, 1999.

change in the overall mass of the system. In contrast, the nucleon mass — and therefore the mass of our macroscopic world — is dominated by the strong confining interaction among the constituents of the nucleon while the bare masses of the constituents contribute only a few percent to the nucleon mass. Because of this sensitivity to the interaction, properties of isolated hadrons — in particular their mass — may be different from those embedded in nuclear matter with many other nucleons nearby. In addition, these properties may be further modified if the nuclear environment is compressed or heated as *e.g.*, in nucleus-nucleus collisions.

In this contribution, experimentally established medium effects in photonuclear reactions will be presented and discussed. The photoproduction of mesons on free and bound nucleons is used as a tool for studying medium modifications of nucleon resonances. These effects may be linked to the in-medium modifications of mesons which feed back on the properties of the decaying states. The effect of the nuclear environment on mesonic properties is also studied in hadron and heavy-ion induced reactions. A corresponding research program at GSI Darmstadt will be described.

2. Photoabsorption on free and bound nucleons

The absorption of photons on free and bound nucleons in the 0.1–2.0 GeV energy regime has been studied by several groups. The experimental results

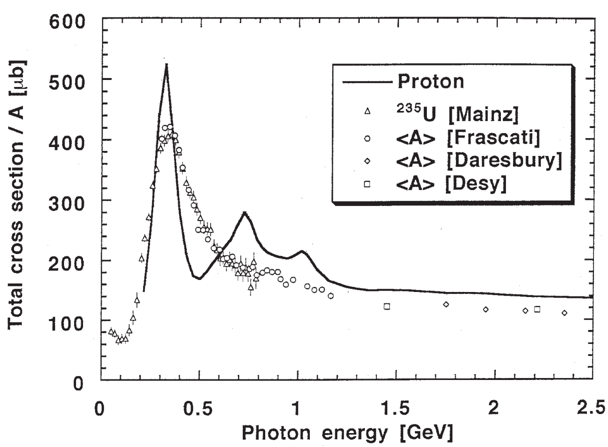

Fig. 1. Comparison of photoabsorption cross sections on free and bound nucleons [1].

are displayed in Fig. 1. As in the Franck–Hertz experiment on atoms, energy can only be transferred to the nucleon in certain portions. The distinct structures in the excitation function on the free proton can thus be associated

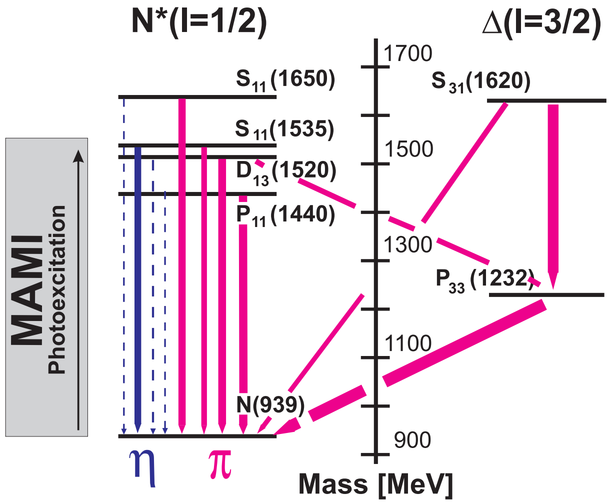

Fig. 2. Excitation energy spectrum of the nucleon. The states are separated according to their isospin. Main decay modes and the excitation energy range accessible at MAMI are indicated.

with excited states of the nucleon. These are the $\Delta(1232)$-resonance, the lowest non-strange excitation of the nucleon, overlapping resonances in the second resonance regime ($P_{11}(1440)$, $D_{13}(1520)$, $S_{11}(1535)$) (see Fig. 2) and still higher lying states in the third resonance regime. Due to meson decay via the strong interaction the resonances are very short lived ($\tau \approx 3\times10^{-24}$s) and correspondingly have widths of the order of 150 MeV. The observation of the Δ resonance in the early 50's was actually the first indication for the composite structure of the nucleon long before the quark-gluon substructure of the nucleon was discovered and studied in deep-inelastic lepton scattering at the end of the 60's.

The cross section per nucleon for photoabsorption on nuclei shows different features. While the structure assigned to the Δ-excitation of a bound nucleon is still clearly pronounced, the bump associated with the second resonance regime is washed out. The photoabsorption on a free and on a bound nucleon are distinctly different, indicating a strong medium effect, a modification of hadronic properties in nuclear matter. To trace the medium modification to individual resonances it is not sufficient to study the inclusive photoabsorption process. Instead, the excitation of the individual resonances in exclusive reactions has to be investigated. Here, the characteristic decay properties of the different resonances can be exploited. The $\Delta(1232)$-resonance decays via single pion emission; the resonance structure is most pronounced in the neutral pion channel since non-resonant contributions (Born-terms) are suppressed. The $S_{11}(1535)$ resonance decays to $\approx 50\%$ into η mesons. Since no other nucleon resonance has a comparably large η branching ratio the observation of an η meson is a characteristic tag on the excitation of the $S_{11}(1535)$ resonance. The $D_{13}(1520)$ resonance has a predominant decay mode into two pions. Most decays occur via subsequent emission of the two pions but some pions are correlated as *e.g.*, in the decay via a ρ meson. In the subsequent sections, these decay properties are used to establish differences in free and in-medium properties of the individual resonances.

3. Experimental approach

This section gives a brief account of the experimental approach to study the photoproduction of mesons with the Two-Arm-Photon-Spectrometer TAPS at the Mainz microtron MAMI. Bremsstrahlung photons are produced by the 880 MeV continuous wave electron beam from MAMI impinging on a

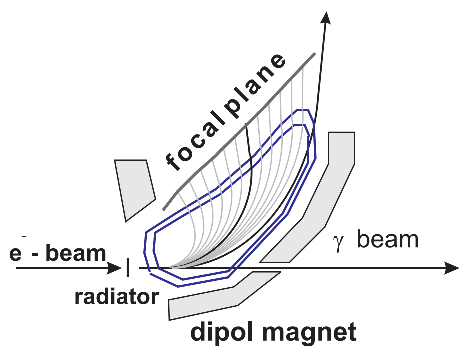

Fig. 3. Energy tagging of bremsstrahlung photons.

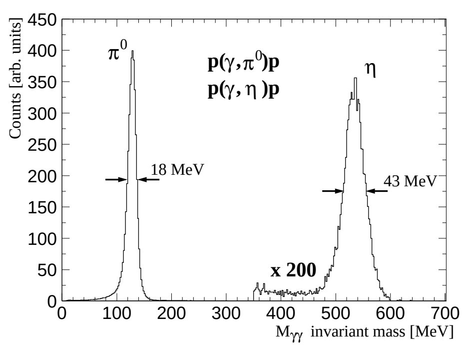

Fig. 4. Invariant mass spectra of photon pairs detected in TAPS.

radiator wire. The photon energy is deduced event-by-event from the energy of the scattered electron measured in coincidence in a magnetic spectrometer (tagger), as illustrated in Fig. 3. After collimation, the bremsstrahlung beam is transported to the nuclear target in an evacuated beam line. Typical photon fluxes are about 500 kHz/(2MeV). The photon energy resolution is about 2 MeV. Neutral mesons produced in the target are detected via their 2γ-decay with the 508 BaF_2-scintillation detectors of the Two-Arm-Photon-Spectrometer TAPS, arranged in the horizontal plane around the scattering chamber in 6 blocks and a forward wall. For each photon pair detected in TAPS the invariant mass is determined. The two photon invariant mass resolution for π^0 and η mesons is illustrated in Fig. 4.

4. Properties of free nucleon resonances

In this section, experimental results on the photoproduction of mesons on the free nucleon are presented.

4.1. Δ(1232) resonance

The cross section for single pion photoproduction on the free proton (see Fig. 5) exhibits a strong peak at a photon energy of 330 MeV which

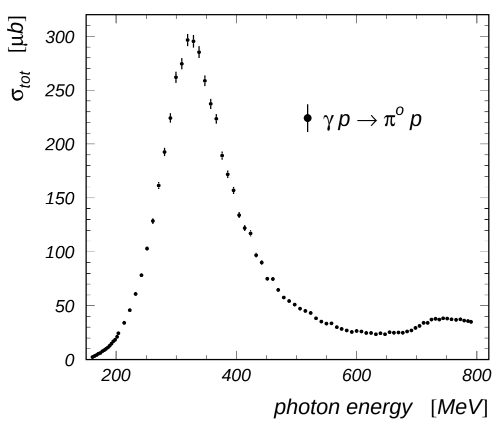

Fig. 5. Cross section for single π^0 photoproduction from the proton. The figure is adapted from [2].

corresponds to the excitation of the $\Delta(1232)$ resonance. The resonance mass and width deduced from the figure are 1230 MeV and 120 MeV, respectively, in agreement with the particle data values. The π_0 angular distribution at the resonance energy (not shown) is consistent with the well known spin $J = 3/2$ of the Δ resonance.

4.2. S_{11}(1535) resonance

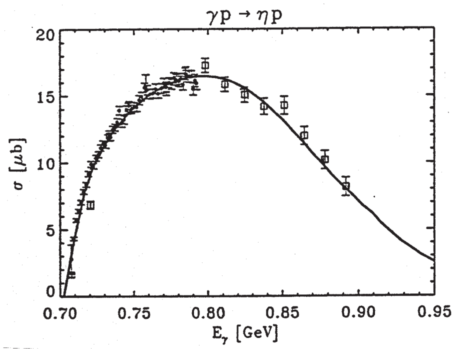

Fig. 6. Cross section for photoproduction of η mesons from the proton. The data are compiled from [3, 4].

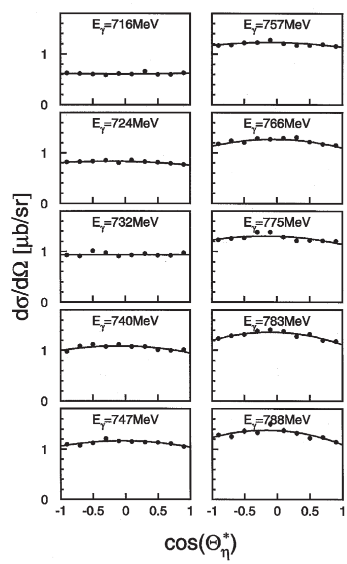

Fig. 7. Angular distribution of η mesons from the $\gamma p \to p\eta$ reaction for different photon energy bins [3].

Fig. 6 shows the excitation function for the photoproduction of η mesons. The steep rise in the cross section is attributed to the presence of the S_{11} resonance with a resonance pole 50 MeV above the η threshold. The η-angular distributions shown in Fig. 7 are almost isotropic at least near threshold, demonstrating the s-wave character of this resonance.

4.3. D_{13} *(1520) resonance*

The cross section for the photoproduction of 2 π_0 mesons rises steeply above E_γ = 400 MeV and peaks at E_γ = 740 MeV (see Fig. 8) which corresponds to $\sqrt{s} = 1510$ MeV, close to the mass pole of the D_{13} resonance.

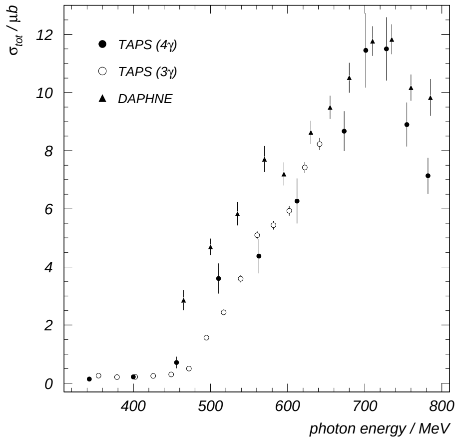

Fig. 8. Cross section for 2 π^0 photoproduction from the proton. The data are taken from [5, 6].

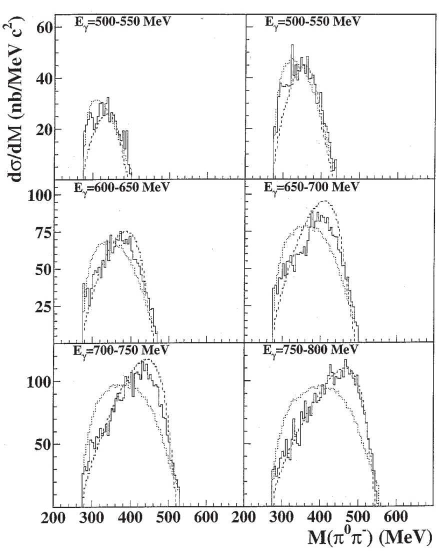

Fig. 9. $\pi^-\pi^0$ invariant mass spectra from the reaction $\gamma n \to p\pi^-\pi^0$. The data are from [7]; the curves represent three-body phase space distributions and the calculations (dashed) are from Ochi *et al.* [8].

A detailed analysis of the three particle exit channel using Dalitz plots has established that the decay occurs predominantely via sequential emission of the two neutral pions with the Δ resonance as an intermediate state [5]. A corresponding analysis of the reaction $\gamma n \to p\pi^-\pi^0$, performed by the DAPHNE group, showed a deviation from equal phase space population in the $\pi^-\pi^0$ invariant mass distribution, indicating a correlation between the two pions as shown in Fig. 9. This deviation from a phase space distribution has been taken as evidence for the emission of a low mass ρ-meson [7] (the ρ resonance has a width of 150 MeV). This experimental observation is corroborated by a recent TAPS measurement of the $\gamma p \to p\pi^+\pi^0$ reaction. A difference between the $\pi^+\pi^0$ — and $\pi^o\pi^0$ — invariant mass distributions has been observed [9]. Since there is no $\rho^0 \to \pi^0\pi^0$ decay this difference can be attributed to a $\rho^+ \to \pi^+\pi^0$ contribution. This is further supported by the $\pi^+\pi^0$ angular distribution. It is, however, not yet clear to what extent the ρ strength can really be attributed to the $D_{13} \to N\rho$ decay or to background terms.

5. Properties of bound nucleon resonances

In this section, experimental results on the photoproduction of mesons from nucleons bound in nuclei are presented.

5.1. Δ(1232) resonance

The excitation of a bound nucleon to the Δ resonance has been studied in the photoproduction of π^0 mesons on ^{4}He and ^{12}C as shown in Figs. 10, 11. In the theoretical analysis of Drechsel *et al.* [11] the interaction of the Δ resonance with the nuclear environment is taken into account by adding a self energy term Σ_Δ in the free Δ-propagator:

$$\frac{1}{W - M_\Delta + i\Gamma_\Delta(W)/2} \Longrightarrow \frac{1}{W - M_\Delta + i\Gamma_\Delta(W)/2 - \Sigma_\Delta}\,. \tag{1}$$

The self energy is parametrized as

$$\Sigma_\Delta(E_\gamma, q^2) = V(E_\gamma)F(q^2), \qquad F(q^2) = e^{-\beta q^2}\,, \tag{2}$$

where V is a complex potential which reflects the medium modification of the Δ resonance and is obtained from a fit to the data. The real and imaginary part of V represent additional contributions to the resonance mass and width, respectively. They are shown in the lower part of Fig. 10. A mass shift of the order of 20 MeV is a small correction ($\approx 2\%$) while the increase in width is of the order of 30%. The remarkable result of the analysis by Drechsel *et al.* is that the same potential parameters also reproduce the

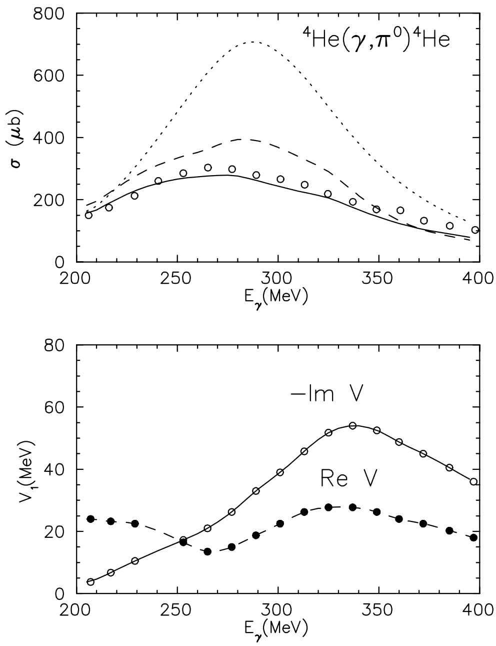

Fig. 10. Energy dependence of the total cross section for the $^4He(\gamma,\pi^0)^4He$ reaction. The experimental data are from [10]; the curves represent PWIA and DWIA calculations and calculations including the Δ self energy term [11]. The corresponding parameters of the potential are given in the lower figure.

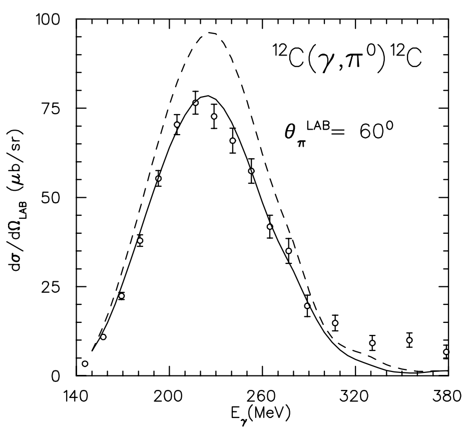

Fig. 11. Energy dependence of the differential cross section for coherent π^0 photoproduction from ^{12}C at $\theta^{\pi^0}_{lab} = 60^0$. The experimental data are from [12], the calculations from [11].

cross section for coherent π^0 production on ^{12}C (see Fig. 11), indicating a saturation of the Δ-nucleus interaction.

5.2. S_{11}(1535) resonance

The in-medium properties of the S_{11} resonance have been studied by measuring the photoproduction of η mesons on nuclei [13, 14]. The exper-

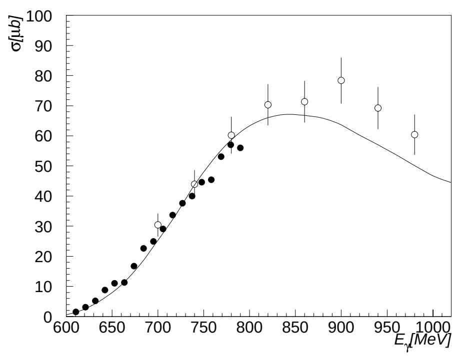

Fig. 12. Energy dependence of the η photoproduction cross section on Carbon. The data are from [13, 14]. The solid curve represents a QMD calculation described in [14].

imental results for ^{12}C are shown in Fig. 12. According to [14] a resonance width of 250 MeV is needed to reproduce the experimental excitation function which again corresponds to an increased width by about 30 - 40 % compared to the free S_{11} width while the resonance mass is hardly effected.

5.3. D_{13}(1520) resonance

The photoproduction of mesons on the free proton in the D_{13} resonance mass range revealed an appreciable ρ-strength (see Section 4). As discussed in Section 6, there is evidence for a strong spreading of the ρ meson strength in the nuclear medium because of its couplings to N*-hole excitations. This would imply a strong increase of the ρ decay width and thus of the total D_{13} width. As a consequence, the opening of phase space for ρ decay of the D_{13} resonance may provide enough resonance broadening to explain the disappearance of structures in the photoabsorption on nuclei. The result of a corresponding transport model calculation [15] is shown in Fig. 13. In this scenario the disappearance of structures in the photoabsorption on nuclei is traced to medium modifications of a vector meson which in a self-consistent treatment have an impact on the in-medium properties of the D_{13} resonance.

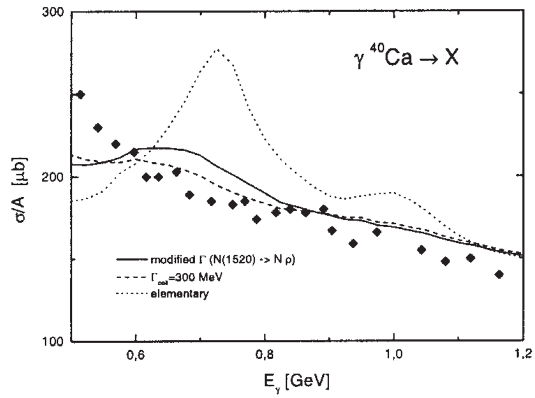

Fig. 13. Photoabsorption cross section in the second resonance region on the proton and on ^{40}Ca in comparison to theoretical calculations [15] taking different in-medium effects into account.

6. Properties of vector mesons in the nuclear medium

Further understanding of the in-medium effects observed in the photoabsorption on nuclei requires a discussion of the current status of vector meson properties in the nuclear medium. Several groups have studied the interaction of ρ mesons with the surrounding nuclear medium (see *e.g.*, [16–18]). All groups consistently find a strong broadening of the ρ spectral function in nuclei at normal density; an example is shown in Fig. 14. Experimental evidence for a lowering of the in-medium ρ mass stems from studies of di-lepton production in heavy-ion collisions at ultra-relativistic energies. Di-leptons are particularly suited as probes of vector meson properties in hadronic mat-

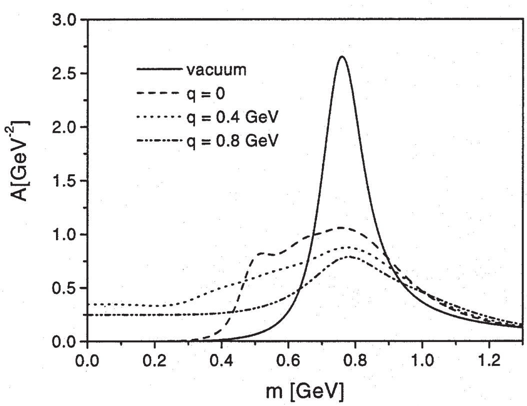

Fig. 14. Spectral function of the ρ meson for different momenta [16].

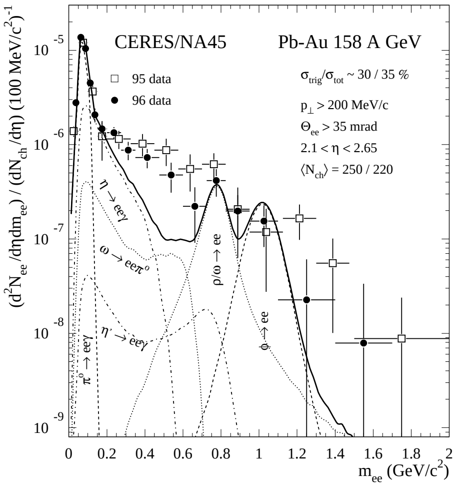

Fig. 15. Inclusive invariant e$^+$e$^-$ mass spectrum in 158 AGeV Pb-Au collisions [19]. The solid curve represents the e$^+$e$^-$ yield from hadron decays. The contributions of the individual decay channels are also shown.

ter since dileptons from vector meson decays can leave the interaction zone with a low rescattering probability. In 158 AGeV Pb+Au collisions, the CERES collaboration has observed unexpectedly high dilepton yields for invariant di-lepton masses in the range between 200 and 600 MeV/c^2 [19] (see Fig. 15). This observation can be accounted for by considering secondary processes such as $\pi^+\pi^- \to e^+e^-$ annihilation if one allows for in-medium changes in the ρ spectral function [20]. Other scenarios like contributions of radiation from a partonic phase in the heavy-ion collision are, however, discussed as well.

The study of vector meson properties in hadronic matter is one of the main goals of the physics program with the dilepton spectrometer HADES (see Fig. 16) which is being installed by a European collaboration at GSI, Darmstadt. The detector system is designed to measure e^+e^- pairs with high acceptance ($\approx$ 40%) and high resolution ($\sigma_M \approx$ 1%) for transverse momenta up to 1.5 GeV/c and invariant masses up to 1.5 GeV/c^2. The experimental program will take advantage of the various beams available from the SIS accelerator, including heavy-ion, proton and secondary π beams. This will allow a study of vector meson properties in hadronic matter over a wide range of baryon densities and temperatures as well as different kinematic conditions.

One of the key experiments will be the study of the ω mass at normal nuclear matter density which, as a free particle, has a rather narrow width of 8 MeV. According to calculations shown in Fig. 17, a shift in mass by

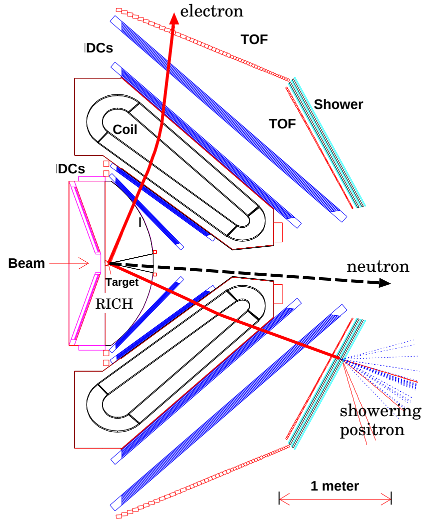

Fig. 16. Schematic diagram of the dilepton spectrometer HADES.

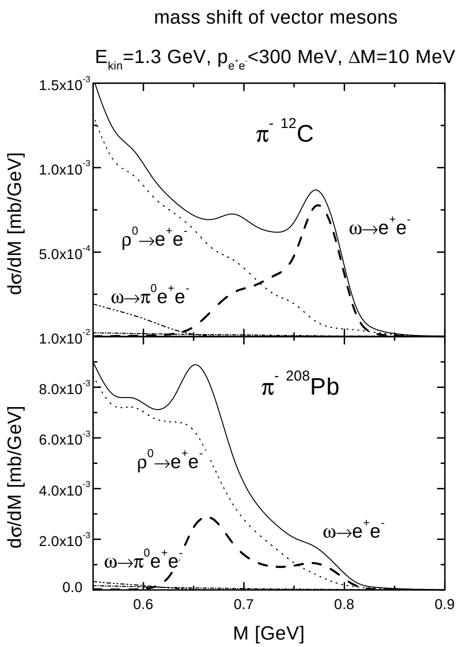

Fig. 17. Predicted dilepton invariant mass spectrum for π induced ω production on nuclei [21].

10–20% is expected. The kinematics of the $\pi^- p \rightarrow n\omega$ reaction on a bound proton allows for almost recoilless ω-production in nuclei which ensures that a high fraction of ω mesons decays within the nucleus. This fraction can be further enhanced by appropriate selections on the ω momentum. The effect of a mass modification is best seen by comparing dilepton spectra from the ω decay in a big and small nucleus as shown in Fig. 17.

7. Summary

The medium effect observed in the photoabsorption on nuclei has been investigated by comparing the properties of free and bound nucleon resonances, studied via the photoproduction of mesons. An intriguing suggestion for the disappearance of structures in the photoabsorption cross section in the second resonance regime may be a broadening of the D_{13} resonance caused by a shift of the ρ strength to lower masses in the nuclear medium. This scenario establishes a direct link between the photo nuclear studies of baryon properties in the nuclear medium and investigations of in-medium hadron properties using heavy-ion and hadron beams.

The results presented in this article are largely based on the work of the TAPS and A2 collaborations at MAMI. I would like to thank the scientists, technicians and in particular the many Ph.D. students who have carried the major load in data taking and analysis. It is a pleasure to acknowledge illuminating discussions with M. Effenberger and U. Mosel. I am grateful to J. Ritman and S. Schadmand for critical comments on the manuscript.

REFERENCES

[1] C. Amsler *et al.*, *Nucl. Phys.* **A622**, 315c (1997).
[2] B. Krusche *et al.*, *Eur. Phys. J.* **A6**, 309 (1999).
[3] B. Krusche *et al.*, *Phys. Rev. Lett.* **74**, 3736 (1995).
[4] B. Schoch, *Prog. Nucl. Part. Phys.* **34**, 43 (1995).
[5] F. Härter *et al.*, *Phys. Lett.* **B401**, 229 (1997).
[6] A. Braghieri *et al.*, *Phys. Lett.* **B363**, 46 (1995).
[7] A. Zabrodin *et al.*, *Phys. Rev.* **C60**, 055201 (1999).
[8] K. Ochi, *et al.*, *Phys. Rev.* **C56**, 1472 (1997).
[9] W. Langgärtner, thesis, Univ. Giessen, 1999.
[10] F. Rambo *et al.*, *Nucl. Phys.* **A660**, 69 (1999).
[11] D. Drechsel *et al.*, *Nucl. Phys.* **A**, in press.
[12] M. Schmitz, Ph.D. thesis, Univ. Mainz, 1996.

[13] M. Röbig-Landau *et al.*, *Phys. Lett.* **B373**, 45 (1996).
[14] H. Yamazaki *et al.*, KEK-Tanashi Symp. Dec. 1998.
[15] U. Mosel, *Prog. Part. Nucl. Phys.* **42**, 163 (1999).
[16] W. Peters *et al.*, *Nucl. Phys.* **A 632**, 109 (1998).
[17] F. Klingl *et al.*, *Nucl. Phys.* **A624**, 527 (1997).
[18] R. Rapp *et al.*, *Nucl. Phys.* **A617**, 472 (1997).
[19] G. Agakichiev *et al.*, *Phys. Lett.* **B422**, 405 (1998).
[20] E.L. Bratkovskaya, W. Cassing, *Nucl. Phys.* **A619**, 413 (1997).
[21] M. Effenberger, Ph.D. thesis, Univ. of Giessen, 1999.